PAM8 WDM Transmission based on a Single Time Lens Source with Geometric Shaping

X. Xu, P. Girouard, M.P. Yankov, M. Galili, L. K. Oxenløwe, P. Guan*
DTU Fotonik, Technical University of Denmark, Ørsteds Plads 343, Kgs. Lyngby, DK-2800, Denmark
*pengu@fotonik.dtu.dk

Abstract: We demonstrate a PAM8 WDM-PON transmission using a single time lens source. Geometric shaping is used to minimize the impact of power-dependent noise. 28×1.5 Gb/s WDM signals are transmitted over 26 km with BER below 3.8×10^{-3}. © 2022 The Author(s)

1. Introduction

The Internet has undergone rapid technological change and global expansion in recent decades. The fast-growing demand for bandwidth-hungry applications, such as video streaming and online backups, and the rise of machine learning and artificial intelligence lead to rapid growth in communication traffic. Hence, the development of the new generation passive optical network (PON) is required imminently. Compared to time-division multiplexing passive optical networks (TDM-PON) [1], the configuration of wavelength-division multiplexing (WDM) PON has advantages of higher data capacity, etc. [2, 3] Nonetheless, the high expense of numerous wavelength transceivers inhibits the implementation of this configuration in reality. Previously, a highly flexible Lens-PON system was proposed using a time lens based TDM-to-WDM conversion [3, 4]. Recently, to increase the capacity and reduce costs of PON systems while maintaining low complexity, a 28×375 Mb/s PAM8 WDM PON transmission was demonstrated based on a single time lens source [5]. We have shown the nonlinear noise that occurs mainly in four-wave mixing (FWM) based time lens optical signal processor can cause significant degradation of generated PAM8 WDM signals.

In this paper, we apply geometric shaping [6] to minimize the influence of nonlinear noise on a PAM8 WDM-PON transmission. 28×1.5 Gb/s PAM8 WDM signals are generated using a single time lens source with geometric shaping, and transmitted over 26 km standard single-mode fiber (SSMF) with BER performance below the hard decision forward-error correction (HD-FEC) threshold 3.8×10^{-3}.

2. Experimental setup

The experimental setup is shown in Fig. 1. The output of a CW laser centered at 1536 nm is RZ-PAM8 modulated by a 40 GHz intensity modulator. To drive the modulator, a 25 GHz arbitrary waveform generator (AWG) with a 2^{17}-1 pseudo random binary sequence (PRBS) is used to generate a 14 GBaud PAM8 electric signal. To facilitate the optical Fourier transformation (OFT) operation, we insert 0.25 ns guard intervals for every 28 TDM tributaries. On the OFT side, an OFT is implemented to achieve a TDM-to-WDM conversion from a 42 Gb/s optical TDM signal with 62.5 ps pulse repetition interval to 28×1.5 Gb/s WDM channels with a 63 GHz channel

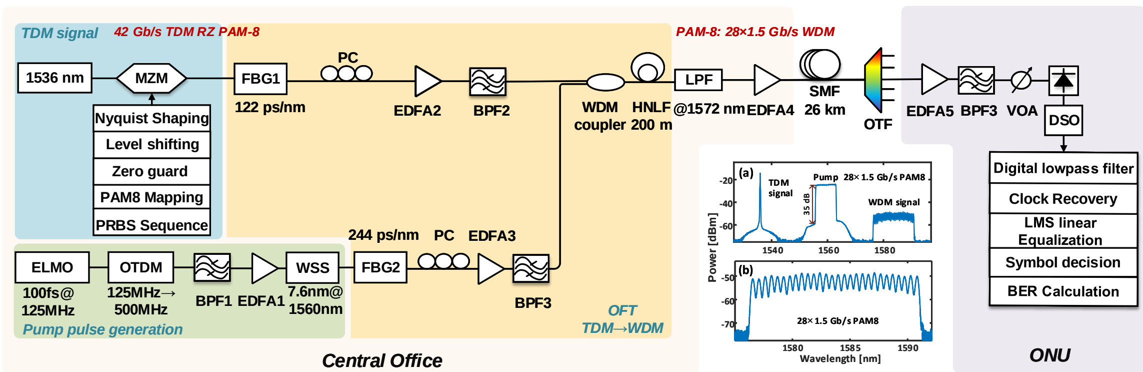

Fig. 1: Experimental setup of 28×1.5 Gb/s PAM8 WDM transmission based Optical Fourier Transformation, inset: (a) The output OFT spectrum at the HNLF output. (b) The output spectrum of the idler.

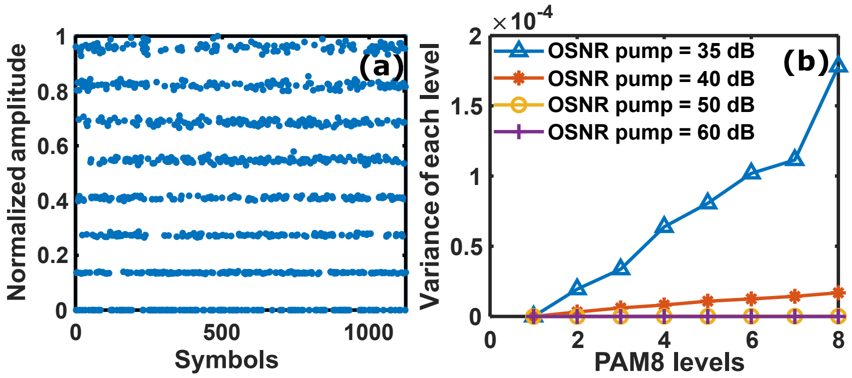

Fig. 2: (a) The symbol sequence of the simulated idler impacted by nonlinear noise after wavelength conversion with pump OSNR of 35 dB, (b) The relationship between the noise variance of each level when the pump OSNR is 35, 40, 50 or 60 dB.

spacing based on time lens, which includes two processes: dispersion and quadratic phase modulation. The phase modulation is implemented by FWM in this experiment. The relation between the accumulated dispersion D_{sig} and the added linear chirp K_{pump} by the pump signal should satisfy the OFT condition ($D_{sig} = 1/K_{pump}$) [7]. A 125 MHz femtosecond mode-locked fiber laser output is time-division multiplexed to generate a pump signal with 500 MHz repetition rate. Then the pump signal is carved into a 7.6 nm rectangular spectrum by a wavelength selective switch (WSS) centered at 1560 nm. The designed Fiber Bragg gratings (FBGs) with negligible third order dispersion (TOD) are used as dispersive elements [8]. FBG1 provides 122 ps/nm dispersion on the data signal at 1536 nm. The pump signal is dispersed by FBG2 with 244 ps/nm at 1560 nm to impart phase modulation with an accumulated dispersion of 158 ps^2 for the generated WDM signal. After amplification, both the dispersed data signal and the dispersed pump signal with 11 dBm and 22.4 dBm average power respectively are launched into a 200 m highly nonlinear fibre (HNLF) for FWM to complete the OFT process. Furthermore, the output OFT spectrum contains the TDM signal, a pump signal and the generated idler, which is depicted in the inset (a) of Fig. 1. The inset (b) of Fig. 1 shows the spectrum of the filtered idler which consists of 28×1.5 Gb/s WDM channels with a channel spacing of 63 GHz. The filtered idler is amplified and transmitted over a 26 km single mode fiber (SMF). After transmission, an optical tunable filter (OTF) is regarded as a demultiplexer to separate the 28 WDM channels in the experiment. The BER performance of the signal is evaluated by a variable optical attenuator (VOA) and a 50 GHz PIN/TIA photodiode after amplification. Although this photodetector has low-level noise, it has a relatively low sensitivity. Therefore, EDFA5 is required after OTF. Moreover, the received signal is collected by a 33 GHz digital storage oscilloscope (DSO) with 80 GSa/s sampling rate for digital signal processing (DSP). The steps of the DSP chain are illustrated in Fig. 1.

3. Results and discussion

Nonlinear noise generated after FWM was observed in the demonstration of a 28 × 375 Mb/s PAM8 WDM PON transmission [5]. To minimize the impact of nonlinear noise on system performance, the nonlinear noise source is explored theoretically. For degenerate FWM, the relation between the power of idler $P_i(t)$, signal $P_s(t)$ and pump $P_p(t)$ can be written as (without noise) [9]:

$$P_i(t) = \eta P_p^2(t) P_s(t) \tag{1}$$

where η refers to the efficiency factor of the FWM process. The amplitude modulation is carried out in this work, therefore only the amplitude noise is considered. We assume that additive white Gaussian noise (AWGN) is considered for each term of Eq. (1) ($P_p^2(t)$ $P_s(t)$ and $P_i(t)$), which can be written as n_{p^2}, n_s and n_i, respectively. The corresponding variance can be expressed as $\sigma^2_{n_{p^2}}$, $\sigma^2_{n_s}$ and $\sigma^2_{n_i}$, where $\sigma^2_{n_{p^2}}$ is proportional to the square of the pump variance $\sigma^2_{n_p}$. It is notice that the pump and signal are independent with each other. Thus the idler variance $\sigma^2_{n_i}$ can be written as [10, 11]:

$$\sigma^2_{n_i} = \eta^2 [\sigma^2_{n_{p^2}} \sigma^2_{n_s} + P_s^2 \cdot \sigma^2_{n_{p^2}} + P_p^4 \sigma^2_{n_s}] \tag{2}$$

If we only consider the pump noise, the idler variance can be simplified by ignoring signal noise:

$$\sigma^2_{n_i p} = \eta^2 P_s^2 \cdot \sigma^2_{n_{p^2}} \tag{3}$$

Eq. (3) indicates that the idler noise is determined by pump noise, which can be estimated by the OSNR. Thus the idler noise based on different pump OSNR could be investigated in simulation. To simplify the complexity

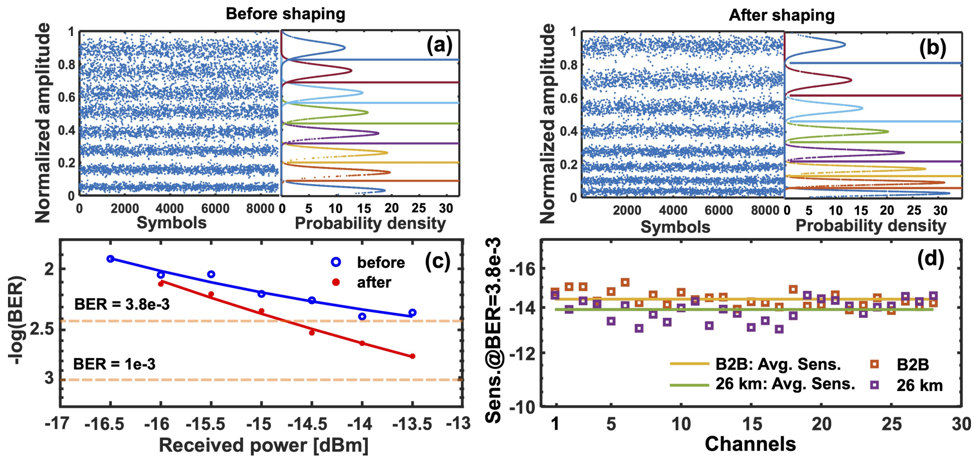

Fig. 3: Both (a) and (b) describe the symbol sequences (left) and the corresponding probability density (right) of the received PAM8 WDM signal in the first channel. (a): before geometric shaping. (b): after geometric shaping. (c) The comparison of the BER performance for a 1.5 Gb/s PAM8 WDM signal in the first channel before (blue curve) and after (red curve) geometric optimization, (d) Received sensitivity of the measured PAM8 signals at BER = 3.8×10^{-3} in all 28 WDM channels.

of simulation, we only simulate the degenerated FWM with two CW laser sources using the split-step Fourier method (SSFM). To be consistent with the experimental parameters, the pump OSNR is set to 35 dB in simulation. A simulated received PAM8 signal with pump OSNR of 35 dB is exemplified in Fig. 2(a). Also, Fig. 2(b) shows the noise variance of the converted PAM8 signal (idler) at each level and different pump OSNRs for a fixed pump power of 10 dBm, indicating that the noise variances is proportional quadratically to the variance of the pump noise, which agrees with Eq. (3). Specifically, when the OSNR of the pump signal is equal to 50 and 60 dB shown in Fig. 2(b), the nonlinear noise can be negligible.

As discussed above, the nonlinear noise originates from the pump noise. In this experiment, particle swarm optimization (PSO) [12] is used to optimize the PAM levels. This process is also known as geometric shaping. Here, the average BER of all levels is used as a cost function to be minimized by the optimizer. The comparison of system performance before and after geometric shaping is illustrated in Fig. 3, indicating that the optimizer pushes the PAM levels closer together at the lower amplitude, where the nonlinear noise is smaller. At the same time, the detectability of the high-levels is increased due to the increased Euclidean distance, leading to on average improved BER. In Fig. 3(c), the blue curve represents the BER performance of the PAM8 signals with the equal-spaced level distribution. The red curve indicates the BER performance of the PAM8 signal with the optimized level distribution. Before optimization, the BER below HD-FEC threshold (BER = 3.8×10^{-3}) cannot be achieved; after optimization, a BER below the FEC threshold performance can be achieved at a received power of -14.67 dBm. Fig. 3(d) shows the receiver sensitivities at BER = 3.8×10^{-3} for all generated PAM8 channels before and after 26 km transmission. The average receiver sensitivity for the back-to-back case is -14.4 dBm, which is 0.5 dB lower than in the transmission case due to short transmission. Moreover, the variation in receiver sensitivity across all 28 channels for the back-to-back case and the transmission case is equal to 1.39 dB and 1.59 dB, respectively, which reveals that the performances of 28 WDM channels are similar.

4. Conclusions

We demonstrate a 28×1.5 Gb/s PAM8 WDM-PON 26 km transmission in SSMF based on the time lens. After geometric shaping, the BER performance have been improved and all 28 WDM channels achieved BER below the HD-FEC threshold.

5. Acknowledgements

VILLUM LENS-PON (19158), DNRF CoE SPOC (DNRF123).

References

1. Derek Nesset. *JOCN*, 9(1):A71–A76, 2017.
2. Dora van Veen. In *OFCC*, pages W1E–2. OSA, 2020.
3. Guan, P. et al. In *CLEO*, pages SM2C–3. OSA, 2018.
4. Guan, P. et al. In *2018 OFC*, pages 1–3. IEEE, 2018.
5. Xu, X. et al. In *2021 CLEO*, pages 1–2. IEEE, 2021.
6. Jones, Rasmus T. et al. In *ECOC*. IEEE, 2018.
7. S. Wabnitz. et al. Springer, Cham, 2015.
8. Xu, X. et al. pages STh3L–4, 2020.
9. Song, S. et al. *JLT*, 17(11):2285–2290, 1999.
10. Leo A Goodman. *JSTOR*, 55(292):708–713, 1960.
11. Anthur, A. P. et al. *JOSA B*, 34(2):389–396, 2017.
12. Kennedy, J. et al. In *ICNN*, volume 4. IEEE, 1995.